Rotation Curves and Bars: Accounting for Non-circular Motions in Barred Spiral Galaxies

Toky H. Randriamampandry[1]**, Claude Carignan**[1]**, Francoise Combes**[2] **and Nathan Deg**[1]

[1]Department of Astronomy, University of Cape Town, Private Bag X3, Rondebosch 7701, South Africa
[2]LERMA, Observatoire de Paris, College de France, PSL, CNRS, Sorbonne Univ., UPMC, F-75014, Paris, France

E-mail: tokyr@ast.uct.ac.za

Abstract. The rotational velocities derived from the gas are often used to study the distribution of the luminous and the dark matter content of disk galaxies by assuming circular gas motions and that disk galaxies are axisymmetric. Unfortunately, this is not the case for barred galaxies since the observed velocities are the combination of an azimuthally averaged circular velocity and the non-circular flows induced by the gas streaming along the bar. The tilted-ring method implemented in ROTCUR is commonly adopted when deriving rotation curves of galaxies, but ROTCUR overestimates/underestimates the rotation velocities when the bar is perpendicular/parallel to the major axis of the disk. The DiskFit algorithm is specifically designed for barred galaxies. Unfortunately, when the bar angle ϕ_{bar} is close to 0 or 90 degrees DiskFit fails due to the degeneracy of the velocity components. We propose a method of correcting rotations based on numerical simulations of galaxies. We correct the rotation curve derived from the tilted-ring method based on a numerical simulation of a galaxy with similar properties and projections as the observed galaxy. NGC 3319 has a bar which is almost aligned with the major axis and it is used as a case study. The correction is obtained from simulations and applied to the observed rotation curve of this particular galaxy. The mass model analysis shows that the two rotation curves give different results for models with either a dark matter halo or using MOND. This shows the importance of correcting for non-circular motions when performing mass model analysis.

Keywords : Cosmology: dark matter – galaxies: kinematics and dynamics – structure – spiral

1. Introduction

The distribution of mass in an axisymmetric galaxy is well constrained by the rotational velocities derived from the gas using the following assumptions: that the gas is moving in circular orbit and the galaxy is axisymmetric. This is largely the case for spiral galaxies, given the very low velocity dispersion in the gas. However, for barred galaxies, part of the observed velocities are due to non-circular motions induced by the gas streaming along the bar (gas moving along the bar).

The tilted ring method [15] is commonly used to derive the rotation curve of galaxies. This method divides galaxies into rings and estimates the velocities and other kinematical parameters for each ring. It has been implemented in the GIPSY [1] task ROTCUR [3]. Accurate modeling has shown that the mass estimates of barred spiral galaxies may be wrong by up to 20% depending on the orientation of the bar relative to the major axis of the galaxy [6] if the tilted ring method is used to derive the rotation.

The publicly available code DiskFit [16] is specifically designed for barred galaxies. It applies a bi-symmetric flow model with fixed phase in the disk plane to the data. DiskFit does not work when the bar is almost parallel to the major or minor axis because of the degeneracy of the velocity components [14].

We propose a method of correcting rotation curves using results from numerical simulations of galaxies. The corrections are obtained from simulation with similar properties and projections as the observed galaxy. In this paper, we use a snapshot with similar properties to NGC 3319. The expected rotation curve (due to the different components:gas, stars and dark matter in the simulation) is calculated from the gravitational potential. The expected circular velocity is given by:

$$< V^2_{expected} >= r < \frac{\partial \Phi}{\partial r} >= r < F_r > \tag{1}$$

where F_r is the radial force from the particles calculated azimuthally on a grid and Φ is the gravitational potential.

The expected rotation curve $V_{expected}$ is then compared with the rotation curve obtained from mock velocities maps downloaded from the GalMer database using ROTCUR. The correction is the difference between the expected rotation curve and the ROTCUR rotation curve in the bar region. We refer the reader to [12] for more details.

NGC 3319 is chosen as a case study. NGC 3319 has a bar which is almost parallel with the major axis (Φ_{bar} = 2 degrees). Mass models using the observed rotation curve and the corrected rotation curve of NGC 3319 are performed to show the effect of the non-circular motion on the results.

The simulation is explained in section 2, and the method and a case study in section 3. Finally the mass model results are discussed in section 4.

2. The simulation

Simulations from the GalMer project [4] are used in this work. The purpose of the GalMer project was to create a database for merging and isolated galaxies using high resolution N-body/hydrodynamic simulations. The GalMer database consists of a large set of Tree-SPH simulation of galaxies spanning a wide range of morphological types and sizes. The snapshot of the giant Sb model (gSb) at the epoch T=500 Myrs is used in this case study. The gSb model was chosen because it has similar bar properties and buge-to-disk (B/D) ratio with NGC 3319. The GalMer database uses a go-on-the-fly algorithm which enables the user to obtain the masses, the velocity maps and other properties for every snapshot. The radial velocities maps are obtained by projecting the velocity components of each particle into a line-of sight (LOS) radial velocity. The pixel size depends on the zoom that is chosen by the user on the online tool (see [4] for details). The LOS radial velocity is

$$V_r = V_X cos\phi cos\theta + V_r sin\phi sin\theta + V_r cos\theta \,, \tag{2}$$

where V_X, V_Y and V_Z are the velocity components for each particle, ϕ and θ are the azimuthal and polar angles respectively The GalMer database does not provide the observed uncertainties for the mock velocity fields. The velocity maps and other properties are publicly available from the GalMer database (http://galmer.obspm.fr).

3. Case study: NGC 3319

NGC 3319 is a barred spiral galaxy located at a distance of 14.3 Mpc. The 21 cm neutral atomic hydrogen (HI) observations were made with the C and D configurations of the Very Large Array (VLA). The data was retrieved from the archive and reduced using the standard AIPS package. More details about the observations and data reductions can also be seen in [9]. Previous studies (e.g [6]) have shown that the inner part of the rotation curve could be underestimated if the bar is aligned with the major axis. Therefore, the observed rotation curve derived from ROTCUR need to be corrected for the non-circular motions before being used for mass model analysis.

The correction was estimated from the simulation by calculating the difference between the expected rotation curve from the gravitational potential and the rotation curve obtained using the tilted ring method applied to a mock velocity field of the simulation downloaded from the GalMer database

(http://galmer.obspm.fr). The snapshot with bulge-to-disk ratio (B/D) and bar properties similar to NGC 3319 was selected for the correction. A B/D=0.24 is found for NGC 3319 from the 3.6 *μm* surface luminosity profile which is comparable with B/D=0.25 (total mass ratio) for the gSb model. The obtained correction was then scaled in terms of velocity using the V_{max} ratio and in terms of radius using the ratio between the disk scale lengths of the model and NGC 3319 (for more details see [12]) before it is added to the observed rotation curve of NGC 3319.

3.1. Mass model

The mass model is done by comparing the observed rotation curves with the quadratic sum of the luminous and dark matter components using a chi-squared minimization technique. The mass models were carried out using the GIPSY tasks ROTMAS and ROTMOD.

For a mass model with dark matter component, the rotation curve is

$$V_{rot}^2 = V_{gas}^2 + V_{*,disk}^2 + V_{*,bulge}^2 + V_{halo}^2 \ , \tag{3}$$

where V_{gas} is the gas contribution, $V_{*,disk}$ the stellar disk contribution, $V_{*,bulge}$ the stellar bulge contribution and V_{halo} is the contribution of the dark matter component.

3.1.1. Gas and stellar contributions The gas contribution was derived from the gas intensity map and the stellar contribution from the IRAC1 3.6 micron surface brightness profile. The method described in [11] was used to convert the luminosity profile into density profile assuming a constant mass-to-light ratio. The result from [5] obtained using chemo-spectrophotometric galactic evolution (CSPE) models are used for the disk and bulge mass-to-light ratios.

A bulge-disk decomposition was performed to obtain the contribution from the bulge to the rotation curve.

3.1.2. Dark matter contributions The dark matter component is calculated from a theoretical density profile. Here, we only use the pseudo-isothermal sphere (ISO) dark matter profile. The ISO density profile is given as

$$\rho_{ISO}(R) = \frac{\rho_0}{1 + \left(\frac{R}{R_c}\right)^2} \ , \tag{4}$$

where ρ_0 is the central density and R_c the core radius of the halo. The velocity contribution of a ISO halo is given by

$$V_{ISO}(R) = \sqrt{4\pi \, G \, \rho_0 \, R_c^2 \left(1 - \frac{R}{R_c} \, atan\left(\frac{R}{R_c}\right)\right)} \ , \tag{5}$$

3.1.3. Mass model with no dark matter component The Modified Newtonian Dynamic or MOND is also considered. Milgrom stipulated that there is no need for DM when fitting galaxies rotation curve if the Newtonian gravity is modified below a critical acceleration a_0 [8]. In the MOND framework, the gravitational acceleration of a test particle is given by

$$\mu(x = g/a_0)g = g_N \ , \tag{6}$$

where g is the gravitational acceleration, $\mu(x)$ is the standard MOND interpolating function and g_N the Newtonian acceleration (see [8] for more details). For the MOND mass model, the rotation curve is

$$V_{rot}^2 = V_{gas}^2 + V_{*,disk}^2 + V_{*,bulge}^2 \cdot \tag{7}$$
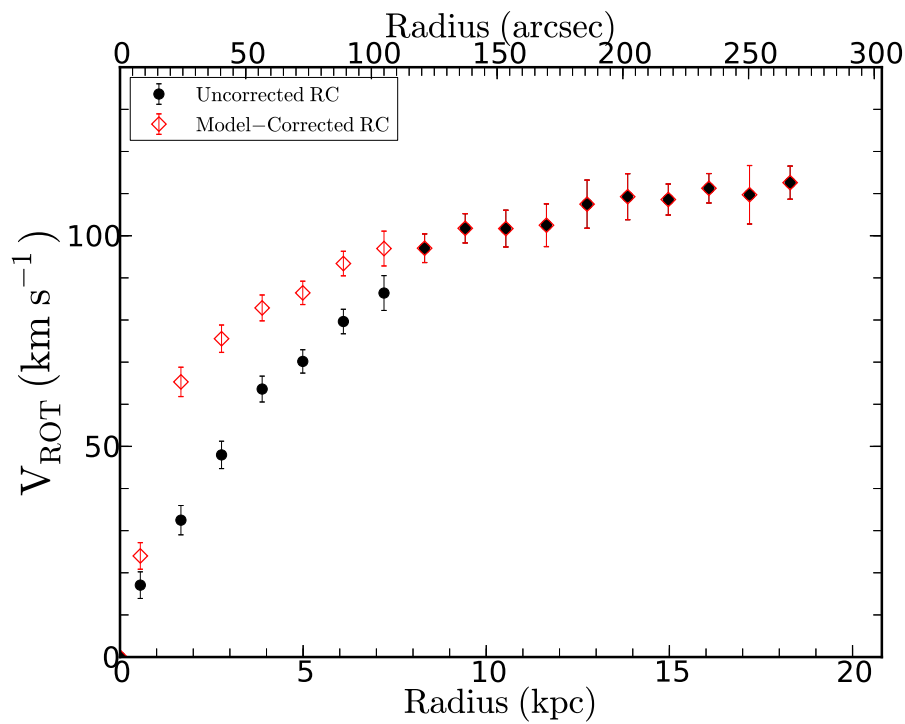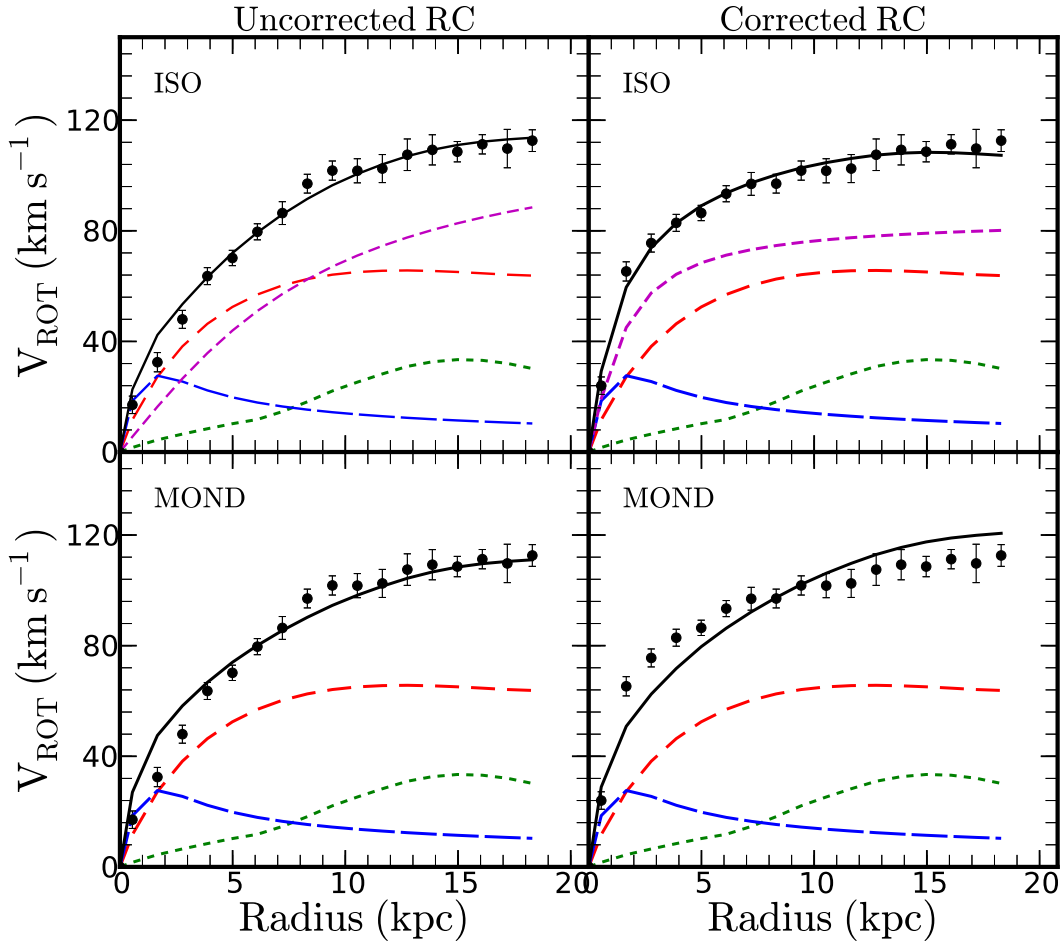
Figure 1. Comparison between the model-corrected and uncorrected rotation curves.

Table 1. Results for the ISO dark matter halo and MOND models using the uncorrected and corrected rotation curves (RCs).

Halo Model	Parameters	Uncorrected RC	Corrected RC
ISO	ρ_0 [a]	5.5±0.9	74.1±15.1
	R_c [b]	6.9±1.1	1.3±0.1
	Υ_d [c]	0.2	0.2
	Υ_b [d]	0.4	0.4
	χ_r^2	1.3	0.7
MOND	a_0 [e]	0.5±0.1	0.7±0.1
	Υ_d [c]	0.2	0.2
	Υ_b [d]	0.4	0.4
	χ_r^2	3.2	5.3

Notes: the central dark matter density [a]ρ_0 is given in units of 10^{-3} $M_\odot$ pc^{-3}, [b] R_c is core radius in kpc , [c]Υ_d is the mass-to-light ratio for the stellar disk, [d]Υ_b for the bulge and [e]a_0 in 10^{-8} cm s^{-2}.

Figure 2. Mass models using ISO DM halo model (top) and MOND model (bottom) for the uncorrected and model-corrected rotation curves. The observed rotation curve is shown as filled black circles with error bars, the gas contribution as dashed green lines, the stellar disk contribution as dashed red lines, the stellar bulge contribution as long-dashed blue lines and the contribution from the dark matter halo as dashed magenta lines. The continuous lines are the best fit model to the rotation curve.

4. Results and Discussions

A comparison between the uncorrected and corrected rotation curves is given in figure 1, where the black circles are the rotation curve obtained from the tilted ring method and the red diamonds are the rotation curve after it has been corrected for non-circular motions.

The mass model results for the uncorrected and corrected rotation curves are presented in figure 2 for the ISO and MOND models and the results are summarized in table 1. For the ISO models, the dark matter halo is much more centrally concentrated when the corrected rotation curve is used, with a $R_C \sim 1$ kpc compared to ~ 5 kpc for the uncorrected rotation curve and a larger ρ_0. It is clear that the corrected and uncorrected rotation curve give very different results for the dark matter parameters. This shows the importance of the non-circular motions on the observed rotation curve and the inferred dark matter properties. The inner part of the rotation curve is under-estimated when the bar is parallel to the major axis, therefore a portion of the mass will be missed if the rotation curve is not corrected and different

conclusions could be drawn from the mass model.

MOND (with constant M/L's) cannot reproduce either the corrected or uncorrected rotation curves. However, even in this case, there is a difference between the inferred a_0's. It is important to note that we are not comparing the goodness-of-fit of the MOND and ISO models. Rather, we are comparing the inferred model parameters using either the corrected or uncorrected rotation curves. The results are significantly different in both cases. This illustrates both the necessity of properly corrected rotation curves for non-circular motions and the promise of using simulations to obtain these corrections for bar-induced motions.

We will be running new simulations of NGC 3319, which will allow us investigated the effect of the orientation of the bar on the observed rotation curve of this galaxy.

Acknowledgments

References

[1] Allen, R. J., Ekers, R. D., Terlouw, J. P., & Vogelaar, M. G. R. 2011, Astrophysics Source Code Library, 9018
[2] Barazza, F. D., Jogee, S., & Marinova, I. 2008, Formation and Evolution of Galaxy Disks, 396, 351
[3] Begeman K. G., 1989, A&A, 223, 47
[4] Chilingarian, I. V., Di Matteo, P., Combes, F., Melchior, A.-L., & Semelin, B. 2010, A&A, 518, A61
[5] de Denus-Baillargeon, M.-M., Hernandez, O., Boissier, S., Amram, P., & Carignan, C. 2013, ApJ, 773, 173
[6] Dicaire, I., Carignan, C., Amram, P., et al. 2008, MNRAS, 385, 553
[7] Kuzio de Naray, R., Arsenault, C. A., Spekkens, K., et al. 2012, MNRAS, 427, 2523
[8] Milgrom M., 1983b, ApJ, 270, 365
[9] Moore, E. M., & Gottesman, S. T. 1998, MNRAS, 294, 353
[10] Navarro J. F., Frenk C. S., & White S. D. M. 1996, ApJ, 462, 563
[11] Oh, S.-H., de Blok, W. J. G., Walter, F., Brinks, E., & Kennicutt, R. C., Jr. 2008, AJ, 136, 2761
[12] Randriamampandry, T. H., Combes, F., Carignan, C., & Deg, N. 2015, MNRAS, 454, 3743
[13] Schoenmakers, R. H. M., Franx, M., & de Zeeuw, P. T. 1997, MNRAS, 292, 349
[14] Sellwood, J. A., & Sánchez, R. Z. 2010, MNRAS, 404, 1733
[15] Rogstad, D. H., Lockhart, I. A., & Wright, M. C. H. 1974, ApJ, 193, 309
[16] Spekkens, K., & Sellwood, J. A. 2007, ApJ, 664, 204